MODELISATION OF TOPOGRAPHIC SITE EFFECT 3D AT THE LOW NOISE UNDERGROUND LABORATORY (LSBB), RUSTREL, FRANCE

E. Maufroy[1], V.M. Cruz-Atienza[1,2], S. Operto[1], O. Sardou[3], G. Sénéchal[4], M. Dietrich[5,6], and S. Gaffet[1,7]

[1] *Laboratoire Géosciences Azur, UMR 6526 UNSA/CNRS/IRD/UPMC, Sophia Antipolis, France*
[2] *Dept. of Seismology, Instituto de Geofísica, Universidad de México, Mexico City*
[3] *Gis Curare, France*
[4] *Laboratoire MIG, UMR 5212 CNRS/TOTAL/UPPA, Pau, France*
[5] *LGIT, UMR 5559 CNRS/UJF/OSUG/IRD/LCPC/Université de Savoie, France*
[6] *Institut Français du Pétrole*
[7] *Laboratoire Souterrain à Bas Bruit, Observatoire de la Côte d'Azur, France*
Email : maufroy@geoazur.unice.fr, gaffet@geoazur.unice.fr

ABSTRACT :

The local geology related to topographic site effects is known to have a strong impact on the amplifications and attenuations of the ground motion. The SHAKE3D finite difference code [Cruz-Atienza *et al.*, 2007] allows studying the influence of various local structures and rheological parameters on the seismic response at the surface. The ground motion is simulated in a realistic heterogeneous 3D model. This model integrates the mountainous topography above the Low Noise Underground Laboratory, Rustrel, France (http://lsbb.unice.fr) and the medium properties deduced from seismic imaging experiment done in 2006.
Such a topography is typical in the South-East region of France : steep slope (greater than 30%) and sharp crest followed by a broad plateau. This configuration also allows investigation of coupled basin-topographic responses at the regional scale.
We consider several models taking into account the spatial variation of the rheological parameters V_P, V_S, Q_P, Q_S, and density together with the topography. Sources with different locations and radiation patterns are also considered relatively to the geometry of the topography. These simulations help us to improve our knowledge of the topographic effects taking into account the heterogeneity of medium and the complexity of the topography.

KEYWORDS : *Site effects, topography, 3D wave propagation, ground motion simulation.*

1. INTRODUCTION

Surface topographies are known to significantly affect the ground motion [Geli *et al.*, 1988; Nechtschein *et al.*, 1995; Bouchon & Barker, 1996; Spudich *et al.*, 1996]. Amplification of seismic waves at the top of hills and ridges is commonly observed from strong earthquakes and seismic recordings [Umeda *et al.*, 1987; Nechtschein *et al.*, 1995; Spudich *et al.*, 1996; Le Brun *et al.*, 1999].
The topographic site effect has been extensively observed and modeled. The best understanding of this phenomena needs a good knowledge of the local surface and underground geology [Assimaki *et al.*, 2005]. Numerical simulations and theoretical works dealing with the ground motion at the top of a topography were often considered from a 2D point of view [Geli *et al.*, 1988; Ashford *et al.*, 1997]. However comparisons between simulated and observed topographic site effects show some disagreements. These disparities can be due to (1) a lack of knowledge on the geological setting, (2) simple wave fields used for the simulations, (3) the 3D effects not being taken into account [Bard & Tucker, 1985; Geli *et al.*, 1988].
The SHAKE3D numerical code for simulations of the ground motion allows propagation of complex wave fields in 3D heterogeneous medium with complex interfaces. Propagation in homogeneous medium overlain by a complex realistic topography allows us to study the influence of the 3D geometry of the topography on the ground motion. We show a statistical spectral ratio method to present the results of these simulations. The mean

amplification factors obtained on top of the topographies can reach important values (commonly 3, 5 to 10 for the sharpest crests), even with an homogeneous media.
Simulations in heterogeneous realistic models will help us to investigate the influence of combined geological and topographic effects.

2. NUMERICAL 3D SIMULATIONS OF THE GROUND MOTION

2.1. The SHAKE3D code

The SHAKE3D finite-difference dynamic-rupture code [Cruz-Atienza & Virieux, 2004; Cruz-Atienza, 2006; Cruz-Atienza *et al.*, 2007] allows studying the influence of various 3D structures and rheological parameters (V_P, V_S, Q_P, Q_S and density) on the seismic response at the surface.
The medium is described by the attribution of the rheological properties values on every node of the numerical grid. The free surface is figured by the null traction conditions and the void properties applied above the interface. A similar way is used to describe the contact between a solid medium and a fluid. Those conditions allow the definition of complex (*i.e.* realistic) geometry interfaces [Cruz-Atienza, 2006].

2.2. Spatial, time and frequency resolutions

The calculation time of our numerical simulations is dependant on the number of nodes in the model, the signal time length and the time resolution. Decreasing these three parameters leads to a reduced calculation time and reduced memory needs. However site effects numerical studies need enough signal time to observe the multiple reflections in the coda. A high spatial resolution is also essential to obtain a coherent signal in the frequencies of concern. From a site effect study point of view, the frequency domain of the results must correspond to the frequency bandwidth where site effects are observed (0.1 to 20 Hz [AFPS, 1993]). These parameters have to be taken into account during the generation of the 3D model, however they strongly increase the calculation time and the memory needs.
The time resolution, *dt*, is dependant on the spatial resolution of the model, *dx*, given by the following formula [Cruz-Atienza, 2006]: $0.7 = V_{max} \times dt / dx$ where V_{max} is the maximum seismic velocity of the model.
The spatial resolution, *dx*, and the minimal seismic velocity, V_{min}, give the maximum frequency where the numeric calculation remains stable. Partly-staggered finite-differences methods, where the free surface is aligned with the reference axis, need 30 points in the time domain per minimal wavelength (N_λ) to be accurate [Bohlen & Saenger, 2006; Cruz-Atienza, 2006]. As an example, for our local homogeneous model (fig. 2C), with $N_\lambda = 30$, $dx = 10$ m and $Vs_{min} = 3000$ m/s, the minimal wavelength is equal to 300 m and the maximum frequency that we can observe is 10 Hz.

3. TOPOGRAPHIC SITE EFFECTS FROM 3D GROUND MOTION SIMULATIONS

3.1. A statistical spectral ratio method

The most classical and commonly used method for the quantification of the site function and especially for the determination of the topographic site effect is the traditional spectral ratio method [Borcherdt, 1970].
It consists in giving the amplification ratio between two stations (classically a site effect station at the crest, and a reference station at the base of the studied topography) in the frequency domain [Field & Jacob, 1995]. The best reference site is commonly defined as a bedrock with an horizontal topography [AFPS, 1993]. However for realistic topographies, such as our local model (fig. 2C), this perfect reference site doesn't exist. Therefore we propose to use a statistical approach instead of using a unique reference point.
In the following examples, we compute spectral ratios for every possible couple of stations, disregarding their location. A statistical amplification factor at one station is obtained by calculating for each frequency the mean value of all the ratios between this station and the others. This method is only accurate for a high number of stations, equally distributed on the surface of interest, this surface incorporating possible site effects but also sites without effect.

This process allows interesting graphic outputs, such as a map of the mean amplification factors in relation to the topography (fig. 1, 2). It is then possible to observe the whole seismic behavior of the zone of interest.

3.2. Source influence

The short variations of the seismic ground motion are exclusively due to site effects where the source distance is much longer than the studied site length. When it is not the case, site effects are still contributing but the differences in propagation path are a part of the observed variations [AFPS, 1993]. A (source distance) / (site to reference distance) ratio equal to 10 is commonly recommended [Field & Jacob, 1995].
To keep reasonable calculation times, a rapid process is to compute two simulations in near field domain with the same source, but one model with the topography and one without. The mean amplification factors from the topographic model, as calculated in 3.1, are then divided by the same factors obtained from the simulation without the topography. The figure 1 illustrates this process.
To simplify the procedure, the SHAKE3D code allows an isotropic excitation point source (a double couple source is also possible, but not shown in this article). An isotropic source avoids directivity effects and radiation patterns, so only the geometric expansion has to be considered.
This isotropic source generates only P-waves, S-waves are created at the interfaces of the model [Cruz-Atienza, 2006]. As homogeneous models have no in-depth interfaces, SV-waves are only generated from the reflection of the P-waves at the free surface [Udías, 1999].

3.3. Homogeneous 3D modeling of the ground motion

3.3.1 Simple topography case

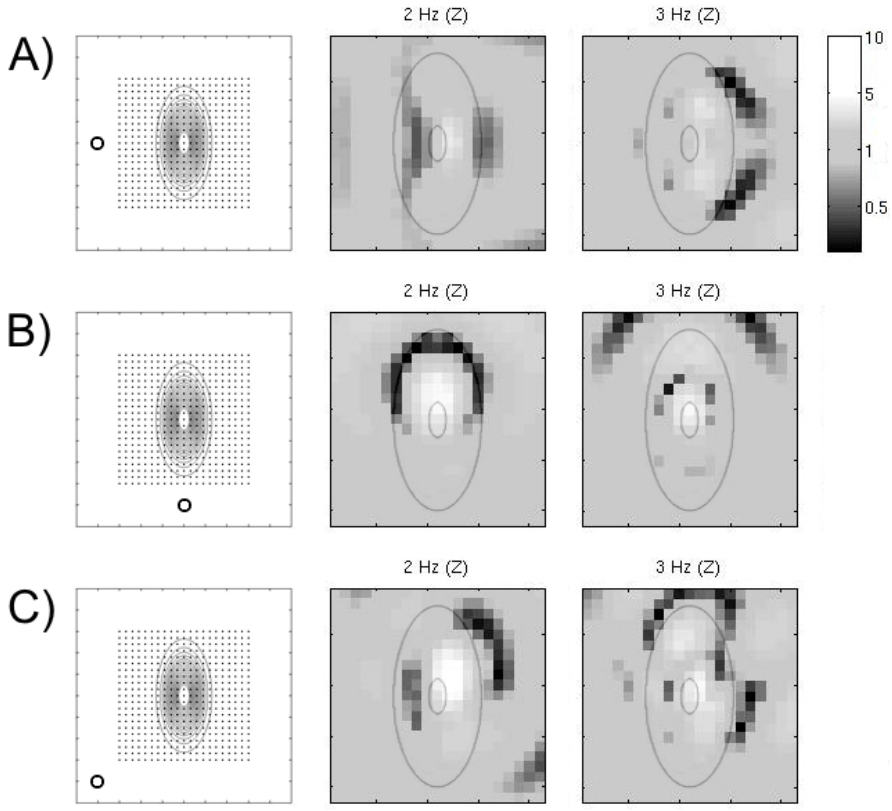

Figure 1 : ***Mean amplification factors for three ground motion simulations with the same topographic model, but three different source locations.*** *Mean amplification factors on centered and right panels are computed as described in 3.1 and 3.2, for respectively 2 and 3 Hz, vertical component. The color bar indicates the values of the mean factors. Model length is 5 km, spatial resolution is 10 m. The source depth is 2 km and the epicenter location (black bold circle) in respect to the topography is shown on the left panels. Small dots show the 441 receivers spread as a square on the elongated topography and on the flat surface. Topography maximum altitude is 700 m. Space between receivers is 150 m.*

2D numerical simulations made by Bouchon [1973] showed that, when the waves are obliquely incident, the zone of amplification on a topography is slightly shifted toward the side of the crest opposite to the upcoming waves (*i.e.* where the incident energy per spatial unit is maximum). We test this configuration for a 3D homogeneous model, an isotropic point source located in three different places, and an artificial elongated topography with a steady slope and a flat summit, as shown on figure 1.

The amplification / deamplification zones on our synthetic cases (fig. 1) have a lobe form distribution. As Bouchon [1973] has shown in 2D numerical simulations, our 3D simulations show that the maximum amplification of the ground motion occur at the opposite crest to the upcoming waves. Zones of deamplification surround all the amplification zones, generally located at the base of the topography or on the closest crest to the upcoming waves. The size of these lobes modifying the spectral amplitude of the seismic waves seems to be frequency dependant.
As we reach the same conclusion as Bouchon [1973], the statistical spectral ratio method described in 3.1 is a correct way to appreciate the topographic site effects.

3.3.2 Realistic topography case

We consider a homogeneous half-space overlain by a realistic topography featuring the topography around and above the Low Noise Underground Laboratory (LSBB, Rustrel, France), which is discretized every 10 m to perform the numerical simulations (fig. 2C). The propagation medium is an elastic material where the seismic velocities are V_P = 5000 m/s and V_S = 3000 m/s.
The source is isotropic, in order to avoid the directivity effects and radiation patterns. This source is tested at different locations, but always deeper than 5 km under the free surface.
Receivers are roughly centered on the model to avoid some possible interferences on the borders of the model due to the possible closeness between the source location and the *Perfectly Matched Layer* (external layer applying energy absorption conditions to simulate an infinite half space and to avoid waves reflection toward the model interior). Receivers are spread on a square pattern, with one station every 100 m (fig. 2A top). Structures of interest, such as North-South and West-East elongated topographies and valleys, are sampled by these receivers (fig. 2).

To understand the impact of the topography increase (*i.e.* smooth slopes and low altitudes *versus* strong slopes and high altitudes) on the ground motion, several models are created from the original local model by applying a factor ranging from 0.1 to 2 on the topography level (fig. 2).
Numerical simulation is processed for each of these 4 topographic models, using the same source for all of them: located in the South-West corner (*i.e.* under the lowest altitudes), 5 km depth, isotropic point. The maximum frequency of these simulations is 10 Hz (N_λ = 30, *dx* = 10 m and Vs_{min} = 3000 m/s).
For the original local model (fig. 2C), the values of the mean amplification factors are coherent with the topography. Amplification occurs at the top of the mountains, the frequency of the maximum amplification is dependant of the dimensions of the topography. The amplification seems to be also dependant on the component considered, but as the source is isotropic, there may be energy on only one horizontal component depending of the location of the receiver in respect to the source point. That is why the elongated topography in the right lower corner of the amplification panels (fig. 2C,D) produces amplification mainly on the X component (there is no much energy on the Y component at this place).
These simulations show that the deamplification in the valleys is of the same magnitude as the amplification on the crests.
For the model on figure 2C, the mean amplification factor can reach 5, but is commonly around 3. The spectral ratio between two stations can easily exceed 10 by considering two extreme receivers, one located at the maximum of the amplification zone, and the reference taken as the deepest point of a valley. This shows the importance of the choice of the reference for field site effect studies. A reference located in the bottom of a sharp valley can lead to marginal spectral ratio values.
The vertical component shows less contrasted factors than the horizontal components, but this may be due to the depth of the source, as it was not the case for the simulations on figure 1, where the vertical component shows the highest amplifications with a superficial source location.

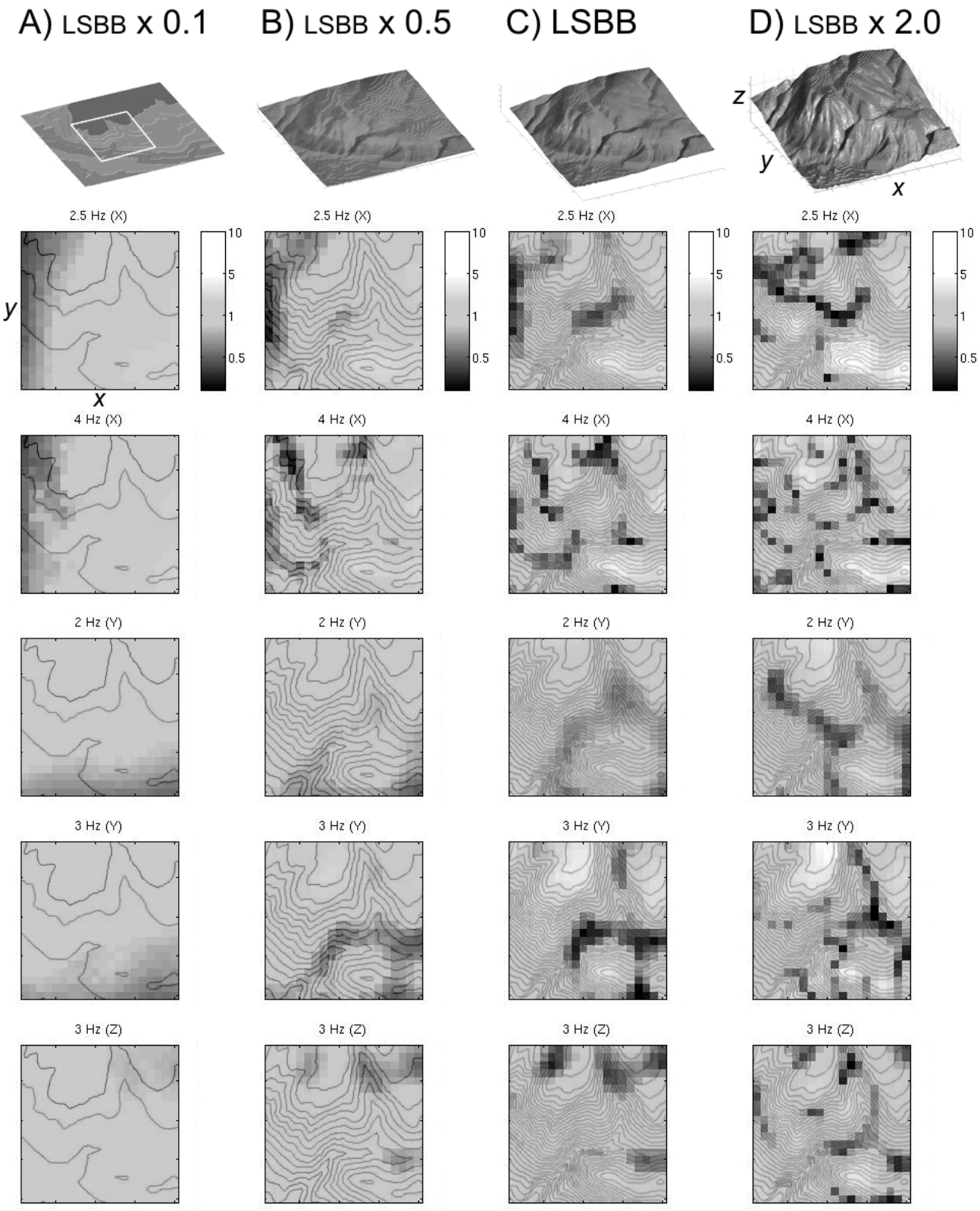

Figure 2 : ***Mean amplification factors for homogeneous models with realistic topography.*** *Mean amplification factors are computed as described in 3.1 and their values are indicated by the color bar. The original topographic model from the LSBB is shown on C. A factor is applied on this topography to create smooth or sharp topographies (A, B, D). Equidistance of contour lines is A) 20 m, B) 20 m, C) 20 m, D) 40 m. Models length is 5 km, spatial resolution is 10 m. Source is isotropic, 5 km depth, located in the South-West corner. Receivers are spread as a square (white square, top A), as described in 3.3.2. Frequency and component are indicated on top of each panel.*

The simulation exposed on figure 2A shows no amplification/deamplification due to the smooth topography. The only visible effect is a decrease of energy due to the source location. The topography is smooth but not flat, however its sharpness is not enough to produce an amplification in the frequencies considered.
Deamplification effects are the first to appear in the model shown on figure 2B. The maximum altitude of this model is around 400 m. This is enough to produce a clear deamplification in the valleys, and a low amplification (maximum 2.8) on the summits.
The sharpest model (fig. 2D) produces the most contrasted mean amplification values (from 0.2 to 8).
The distribution of the factors are slightly different from one model to an other, even if amplification always occur on positive relief and deamplification on negative relief. This confirms the dependence of the amplification location in space and in frequency on the dimensions of the topography.

The influence of the source location described in 3.3.1 has been tested on the realistic model shown on figure 2C. As the results from this complex topographic model lead to the same conclusion as in 3.3.1, the mean amplification factors obtained with different source locations and model on figure 2C are not shown in this article.

4. TOWARDS HETEROGENEOUS 3D MODELING OF THE GROUND MOTION

We have shown that the geometry of the topography has a strong influence on the seismic ground motion. Next we study the influence of combined geological and topographic effects. The SHAKE3D code allows numerical simulations in heterogeneous models which help to understand the impact of the variation of the rheological parameters V_P, V_S, Q_P, Q_S and density on the ground motion.

4.1. Geological setting of the LSBB and Interimages 2006 experiment

To help us generate a realistic 3D heterogeneous model, we gather geological and seismological data from the Low Noise Underground Laboratory (LSBB), Rustrel, France.
The galleries of the LSBB are buried in the south foot of the Albion plateau, a part of a vast karst system (fig. 3). The saturated zone of the karst, the Fontaine-de-Vaucluse aquifer, lies about 200 m below the underground Laboratory [Gaffet *et al.*, 2003]. The figure 3 presents the seismic imaging ([Maufroy *et al.*, 2007], inversion code by Operto S.) of the unsaturated area located above the aquifer, between the LSBB galleries and the topographic surface. This imaging work is part of the Interimages 2006 experiment.
This 2D seismic profile is well correlated with the data from the preliminary geological study [S.S.B.S. program, 1965] (fig. 3). They allow to identify two different ages of limestone: Barremian and Bedoulian, different in their inner fracturing. They show that the area is affected by two sub-vertical fault systems (fig. 3).

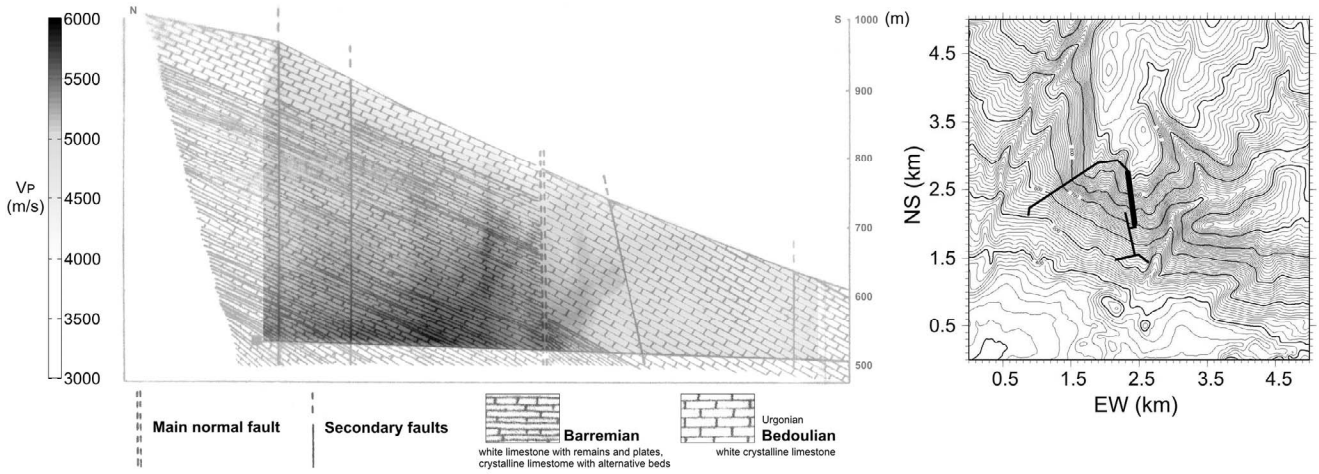

Figure 3 : ***Preliminary geological study*** **[S.S.B.S program, 1965]** ***related to the smooth P-velocity 2D model elaborated from the inversion of the transmission and direct P-wave propagation times [Interimages 2006 experiment; inversion code by Operto S.].*** *On the right, map showing the LSBB underground gallery (black bold line) and its topographical surroundings* [Gaffet *et al.*, 2003]. *Largest bold line shows the emplacement of the Interimages 2006 seismic profile.*

Several realistic 3D heterogeneous models will be elaborated, with more or less complexities. They will integrate the mountainous topography above the Laboratory and the medium properties deduced from the seismic imaging experiment added to the geological and geomechanical preliminary studies.

4.2. Preliminary heterogeneous 3D modeling at the LSBB

A preliminary simple but heterogeneous 3D model of the LSBB is generated (fig. 4). The P-waves velocities of the superficial formations are defined from the Interimages 2006 seismic data. These are mean values, and can be slightly modified to obtain a rapid or a slow model.

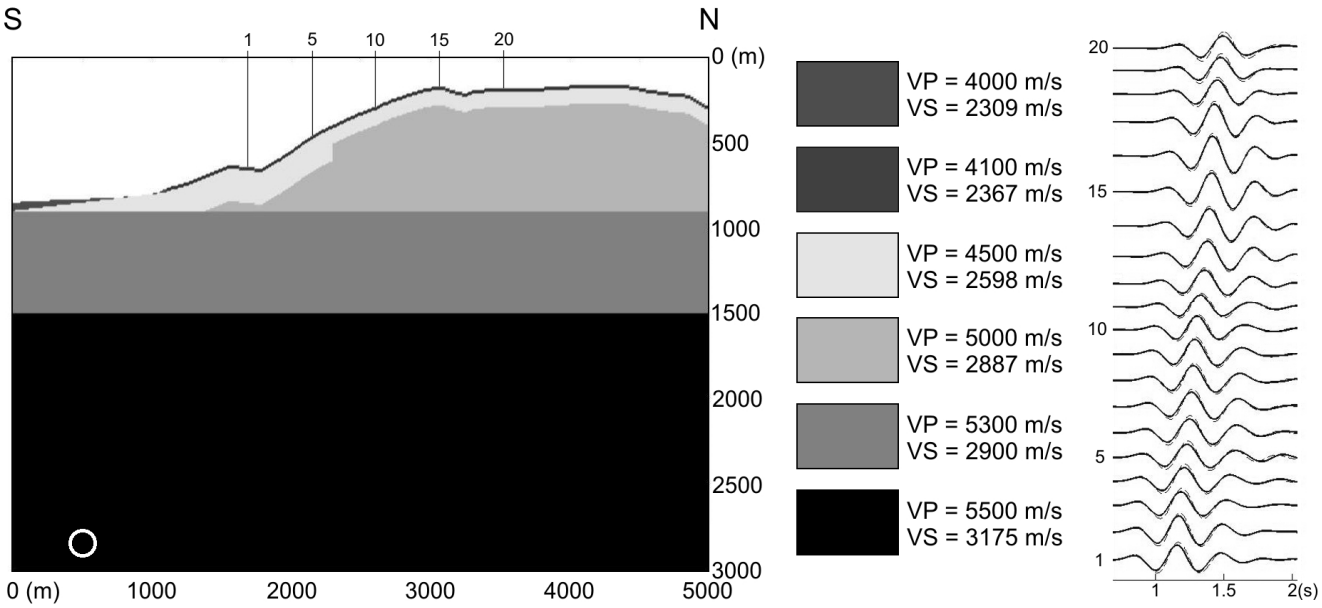

Figure 4 : ***2D profile of the 3D preliminary heterogeneous model of the LSBB and associated propagation waveforms.*** *This heterogeneous model contains 6 layers with different seismic velocities. The white circle shows the projection of the isotropic source hypocenter. Numbers on the profile indicates the location of 20 receivers, which velocity waveforms (NS horizontal component) are shown on the right side. Waveforms from the equivalent homogeneous simulation are plotted in dashed lines.*

This simple heterogeneous model (fig. 4) does not produce higher or differently located mean amplification factors than the equivalent homogeneous model, so a representation of these factors are not shown in this article. The amplification due to the topography is visible on the waveforms amplitudes, which are larger around the 15th receiver located on a surface perpendicular to the incident waves.
As shown on figure 4, the velocity contrasts in this heterogeneous model are not enough to produce a consequently different signal than from an homogeneous model. Signal amplitudes are slightly lower for the heterogeneous simulation, and a small phase delay can be noticed between the two.

5. CONCLUSION AND PERSPECTIVES

The 3D simulations shown in this article illustrate some characteristics of the topographic site effects. The deamplification phenomena in the valleys has the same magnitude as the amplification on the crests. This has important implications for the choice of a correct reference site for field studies. An homogeneous 3D realistic topographic model is enough to produce mean amplification factors reaching 5, which shows the strong impact of the geometry of the free surface on the ground motion, even with no geological particularity.
The location of the maximum amplification in the frequency domain was not approached in this article. However it clearly appears that the spatial dimensions of the topography have a strong influence on the frequency bandwidth of the amplification.

The heterogeneous models, which are part of an ongoing work, will help us to define the role on the ground motion of the rheological parameters combined with the topography.

ACKNOWLEDGEMENTS

Participants to the material for the seismic part of the Interimages 2006 experiment are: IHR ("*Imagerie Haute Résolution*") INSU/CNRS seismic mobile network for the surface sensors; Universities of Pau, Orsay, Grenoble and Toulouse (France) for the gallery seismic geophones; CETE (Nice, France) for the summit array; LSBB underground array. This work is supported by LSBB, University of Nice Sophia Antipolis (France), Geosciences Azur and Seiscope.

REFERENCES

AFPS (Association Française du Génie Parasismique) (1993), Guide méthodologique pour la réalisation d'études de microzonage sismique.

Ashford S.A., Sitar N., Lysmer J., and Deng N. (1997), Topographic effects on the seismic response of steep slopes, *Bull. Seism. Soc. Am.*, **87.3**, 701-709.

Assimaki D., Gazetas G., and Kausel E. (2005), Effects of local soil conditions on the topographic aggravation of seismic motion: parametric investigation and recorded field evidence from the 1999 Athens earthquake, *Bull. Seism. Soc. Am.*, **95.3**, 1059-1089.

Bard P.-Y., and Tucker B.E. (1985), Underground and ridge site effects: a comparison of observation and theory, *Bull. Seism. Soc. Am.*, **75.4**, 905-922.

Bohlen T., and Saenger E.H. (2006), Accuracy of heterogeneous staggered-grid finite-difference modeling of Rayleigh waves, *Geophysics*, **71.4**, T109-T115.

Borcherdt R.D. (1970), Effects of local geology on ground motion near San Francisco Bay, *Bull. Seism. Soc. Am.*, **60**, 29-61.

Bouchon M. (1973), Effect of topography on surface motion, *Bull. Seism. Soc. Am.*, **63.3**, 615-632.

Bouchon M., and Barker J.S. (1996), Seismic response of a hill: the example of Tarzana, California, *Bull. Seism. Soc. Am.*, **86.1A**, 66-72.

Cruz-Atienza V.M. (2006), Rupture dynamique des failles non-planaires en differences finies, *Ph.D. thesis, University of Nice Sophia-Antipolis*.

Cruz-Atienza V.M., and Virieux J. (2004), Dynamic rupture simulation of nonplanar faults with a finite difference approach, *Geophys. J. Int.*, **158**, 939-954.

Cruz-Atienza V.M., Virieux J., and Aochi H. (2007), 3D finite-difference dynamic-rupture modeling along non-planar faults, *Geophysics*, **72.5**, SM123-SM137.

Field E.H., and Jacob K.H. (1995), A comparison and test of various site-response estimation techniques, including three that are not reference-site dependant, *Bull. Seism. Soc. Am.*, **85**, 1127-1143.

Gaffet S., Guglielmi Y., Virieux J., Waysand G., Chwala A., Stolz R., Emblanch C., Auguste M., Boyer D., and Cavaillou A. (2003), Simultaneous seismic and magnetic measurements in the Low-Noise Underground Laboratory (LSBB) of Rustrel, France, during the 2001 January 26 Indian earthquake, *Geophys. J. Int.*, **155(3)**, 981-990.

Geli L., Bard P.-Y., and Jullien B. (1988), The effect of topography on earthquake ground motion: a review and new results, *Bull. Seism. Soc. Am.*, **78.1**, 42-63.

Le Brun B., Hatzfeld D., Bard P.-Y., and Bouchon M. (1999), Experimental study of the ground motion on a large scale topographic hill at Kitherion (Greece), *J. Seismol.*, **3**, 1-15.

Maufroy E., Ribodetti A., Sénéchal G., Zeyen H., Dietrich M., Operto S. and Gaffet S. (2007), Seismic imaging for topographic site effect modeling at the Low Noise Underground Laboratory (LSBB), Rustrel, France, *European Geosciences Union, Vienna*, *Geophysical Research Abstracts*, **9**, 03807.

Nechtschein S., Bard P.-Y., Gariel J.C., Meneroud J.P., Dervin P., Cushing M., Gaubert C., Vidal S., and Duval A.-M. (1995), A topographic effect study in the Nice region, *Proceedings of the fifth International Conference on Seismic Zonation, Nice, France*, 1067-1074.

Spudich P., Hellweg M., and Lee W.H.K. (1996), Directional topographic site response at Tarzana observed in aftershocks of the 1994 Northridge, California, earthquake: implications for mainshock motions, *Bull. Seism. Soc. Am.*, **86.1B**, S193-S208.

S.S.B.S. program (1965), Etude géologique préliminaire du P.C. de la Grande Montagne.

Udías A. (1999), Principles of seismology, *Cambridge University Press*, 475 pp.

Umeda Y., Kuroiso A., Ito K., and Muramatu I. (1987), High accelerations produced by the Western Nagano Prefecture, Japan, earthquake of 1984, *Tectonophysics*, **141**, 335-343.